

Wettability and corrosion of TiN, TiN–BN and TiN–AlN by liquid steel

A. Amadeh^{a,*}, S. Heshmati-Manesh^a, J.C. Labbe^b, A. Laimeche^b, P. Quintard^b

^a*Metallurgy and Materials Department, Faculty of Engineering, Tehran University, Tehran, Iran*

^b*LMCTS (C.N.R.S. URA 320), Université de Limoges, Limoges, France*

Received 15 January 2000; received in revised form 13 May 2000; accepted 13 June 2000

Abstract

The wettability and corrosion behaviour of titanium nitride by liquid steel has been studied. Due to its thermodynamic stability and low solubility in liquid iron, TiN has a good resistance to corrosion by liquid steel. However, its good wettability promotes adhesion to steel. Also, the effects of BN and AlN addition to TiN on the wetting parameters and the mechanisms of the ceramic corrosion by liquid steel have been investigated. © 2001 Elsevier Science Ltd. All rights reserved.

Keywords: AlN; BN; Corrosion; Steel; TiN; Wetting

1. Introduction

Nitride ceramics have excellent potential to become important materials in certain parts of the steel making industry. At present, a great deal of research work is concentrated on evaluating and optimising the properties of these ceramics to make use of them in steel making.^{1,2} Generally, a ceramic material should have a number of properties to indicate a good resistance to corrosion by liquid steel. These include good thermodynamic stability, low solubility in liquid iron and low reactivity with the elements present in steel. Titanium nitride is one of these ceramics which has a number of attractive properties. Regarding the solubility in liquid iron, calculations have indicated that^{3,4} titanium nitride is 10 times less soluble than boron nitride and 5 times less than aluminium nitride (Table 1).

In this work, the wettability and corrosion behaviour of pure TiN in contact with liquid steel have been studied. Also, an attempt has been made to optimise these behaviours by the addition of BN and AlN.

2. Experimental

The compositions of the steel samples used in this work and designated A (low carbon), B (Si–Ca treated) and C (ultra low carbon) are shown in Table 2.

Ceramic substrates were prepared from pure TiN, mixtures of TiN–BN (10 wt.% BN) and TiN–AlN (10, 25 and 50 wt.% AlN). The substrates were hot pressed in a graphite die in the form of cylindrical disks with a diameter of 35 mm and thickness of 3–4 mm. The sintering pressure was chosen considering the maximum strength of the graphite die (35 MPa). The sintering condition and densification of the prepared samples are summarised in Table 3.

The contact angle of the solid ceramic with the liquid steel was measured by sessile drop method at 1550 and 1570°C using the instrumentation described elsewhere.⁵

The major methods employed to study the solid–liquid interfaces of the cooled samples include scanning electron microscopy (SEM) and Raman spectroscopy.

3. Results

3.1. Interaction of steel samples with pure TiN

3.1.1. Contact angle

In the case of steels A and C, the contact angle becomes practically stable in 10 min (Fig. 1), but, in the case of steel B, the angle is stabilised after 40 min and at a low value of θ (considerably less than 90°). This wetting behaviour of steel B distinguishes it from the two others.

3.1.2. Solid–liquid surface tension

The solid–liquid surface tension (σ_{SL}) may be calculated by assuming a constant value for the solid–vapour

* Corresponding author. Tel.: +98-21-8006-076; fax: +98-21-8006-076.

surface tension (σ_{SV}) at a constant temperature. This allows us to evaluate the approximate trend of changes in σ_{SL} with time (Fig. 2). Generally, σ_{SL} decreases with time and is stabilised after 10–15 min.

3.2. Interaction of steel B/TiN–BN

To alleviate the strong adhesion of steel B to the ceramic substrate and the possibility of capillary penetration BN was added to the TiN matrix. It has been reported that the addition of BN to AlN increases the contact angle.² Contrary to what was expected, the addition of BN caused the complete spreading of the molten steel over the substrate ($\theta \cong 0^\circ$). This phenom-

Table 1
Solubility of nitrides in liquid iron at 1600°C

Ceramic	AlN	BN	TiN	Si ₃ N ₄
Solubility (mol/l)	0.21	0.45	0.041	1.29

Table 2
Chemical composition of steels (in ppm)

Steels	A	B	C
C	430	809	41
Si	120	3440	130
Al	450	310	300
Ti	0	20	690
N	46	32	22
Mn	1940	13 960	1340

Table 3
Sintering conditions of the ceramic substrates

	TiN	TiN–BN	TiN–AlN	AlN
T (°C)	1600	1650	1820	1820
P (MPa)	33	33	33	23
t (min)	60	60	60	60
Densification percentage (%)	92	87	95	97

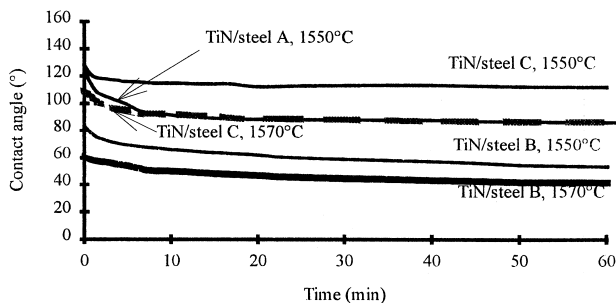


Fig. 1. Contact angle (θ) as a function of time.

enon was accompanied by a gas release which made measurement of the wetting angle difficult.

3.3. Interaction of steel B/TiN–AlN

3.3.1. Wetting angle

The addition of AlN to TiN matrix increases the steel–ceramic contact angle and hinders the wettability (Fig. 3). This trend is more remarkable at 1550 than 1570°C.

3.3.2. Solid–liquid surface tension

Considering the solid–vapour tension of pure AlN as $1000 \pm 100 \text{ J/m}^2 (\times 10^{-3})$ ^{6,7} and that of TiN as $1400 \text{ J/m}^2 (\times 10^{-3})$,⁶ a constant value of $1200 \text{ J/m}^2 (\times 10^{-3})$ was assumed for TiN–AlN mixture to evaluate the solid–liquid surface tension. The variation of σ_{SL} with time indicates that it passes through a minimum and then remains constant (Fig. 4).

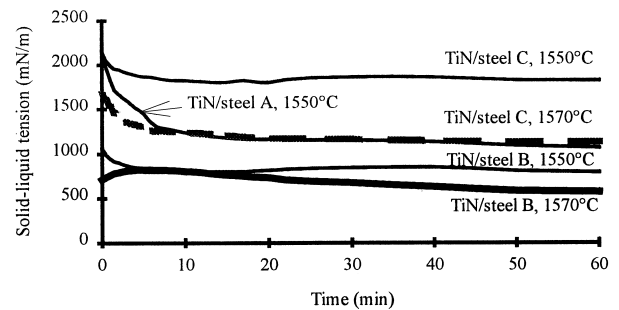


Fig. 2. Solid–liquid surface tension (σ_{SL}) as a function of time.

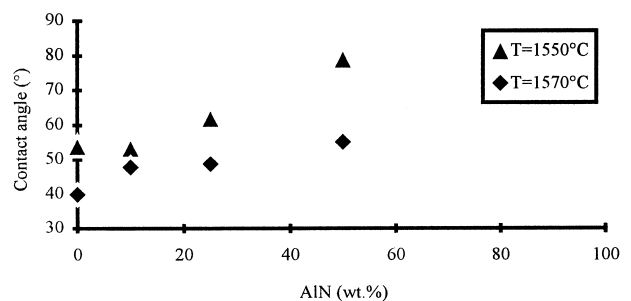


Fig. 3. Variation of θ as a function of AlN content in the TiN matrix.

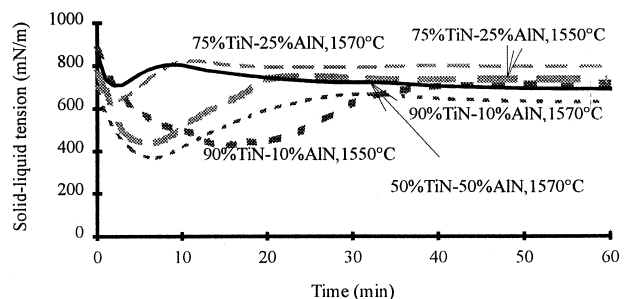


Fig. 4. Variation of σ_{SL} with time.

3.4. Solid–liquid interface studies

The examination of the solid–liquid interfaces with SEM indicated that dissolution of TiN by the liquid steels was practically negligible (Fig. 5). However, the SEM–EDX microanalysis of TiN–AlN interfaces revealed the existence of iron and the depletion of aluminium in a depth of 60, 90 and 55 μm in the substrates containing 10, 25 and 50% AlN, respectively, after being in contact with the liquid steel for 1 h at 1550°C (Fig. 6). Raman spectroscopy confirmed these observations showing the absence of the AlN characteristic bands in a depth of some tens of microns (Fig. 7).

3.5. Corrosion studies by dip test

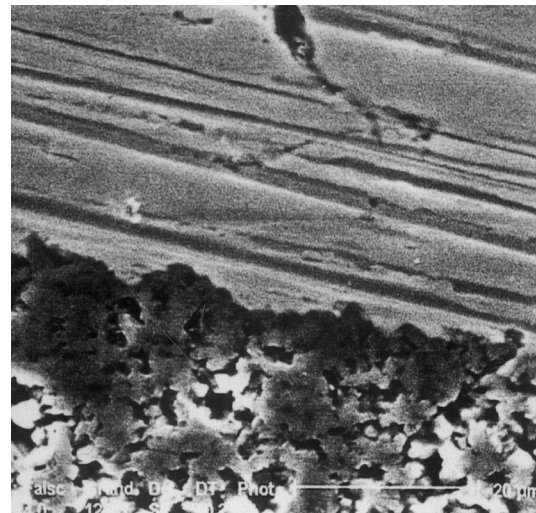
This method consists of introducing the small ceramic bars into a liquid metal bath. The experiments were performed on the small bars with a thickness of 3 mm in contact with the liquid steel for 2, 5, 10 and 20 h at 1550°C in an argon atmosphere. The bars were immersed in the liquid steel to compare the corroded layer with the remaining intact part. The results, summarised in Table 4, indicate the strong resistance of TiN to dissolution in the liquid steel. In the case of TiN–AlN mixtures, the corroded layer is represented by presence of the iron in the solid ceramic bars. The SEM–EDX microanalysis of the intact layer of the ceramic bars revealed the presence of both TiN and AlN compounds, whereas the corroded layer showed presence of TiN, absence of AlN and diffusion of iron into the ceramic bar.

4. Discussion

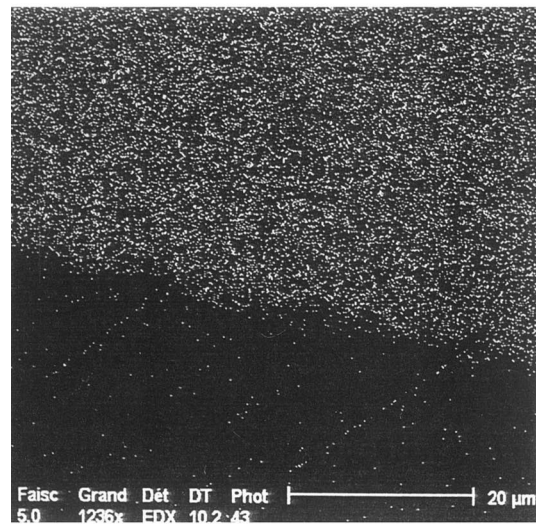
4.1. TiN

The variation of the contact angle between the pure TiN and different steels indicated a continuous reduction with time (Fig. 1) and the equilibrium condition was attained quickly in 10 to 15 min. This behaviour testifies the absence of any chemical interaction between the liquid steel and TiN. The variations of σ_{SL} as a function of time (Fig. 2) confirms this interpretation as the curves do not indicate any minimum value.⁸

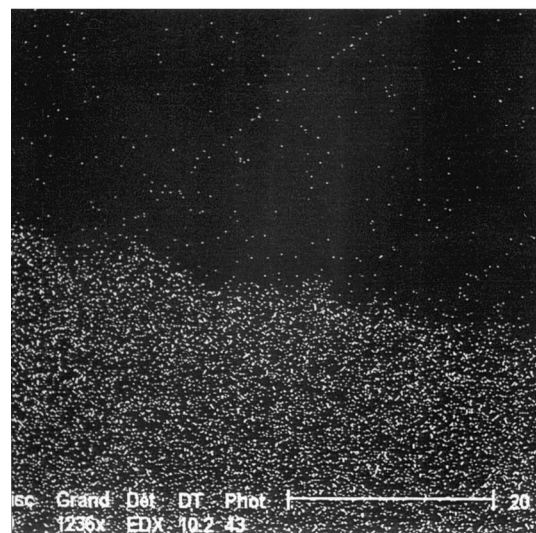
Previous studies on behaviour of pure AlN,¹ AlN–BN and AlN–C² against liquid steels have shown that the corrosion of nitride ceramics takes place via dissolution of nitrides in liquid steel. Also, the dissolved oxygen in steel plays an important role in the evolution of the contact angle and more generally in dissolution of the nitride ceramics by steels. This process may be interpreted according to the following mechanisms:



(a)



(b)



(c)

Fig. 5. Microstructure of (a) the steel B/pure TiN interface; (b), Fe X-ray map; (c) Ti X-ray map.

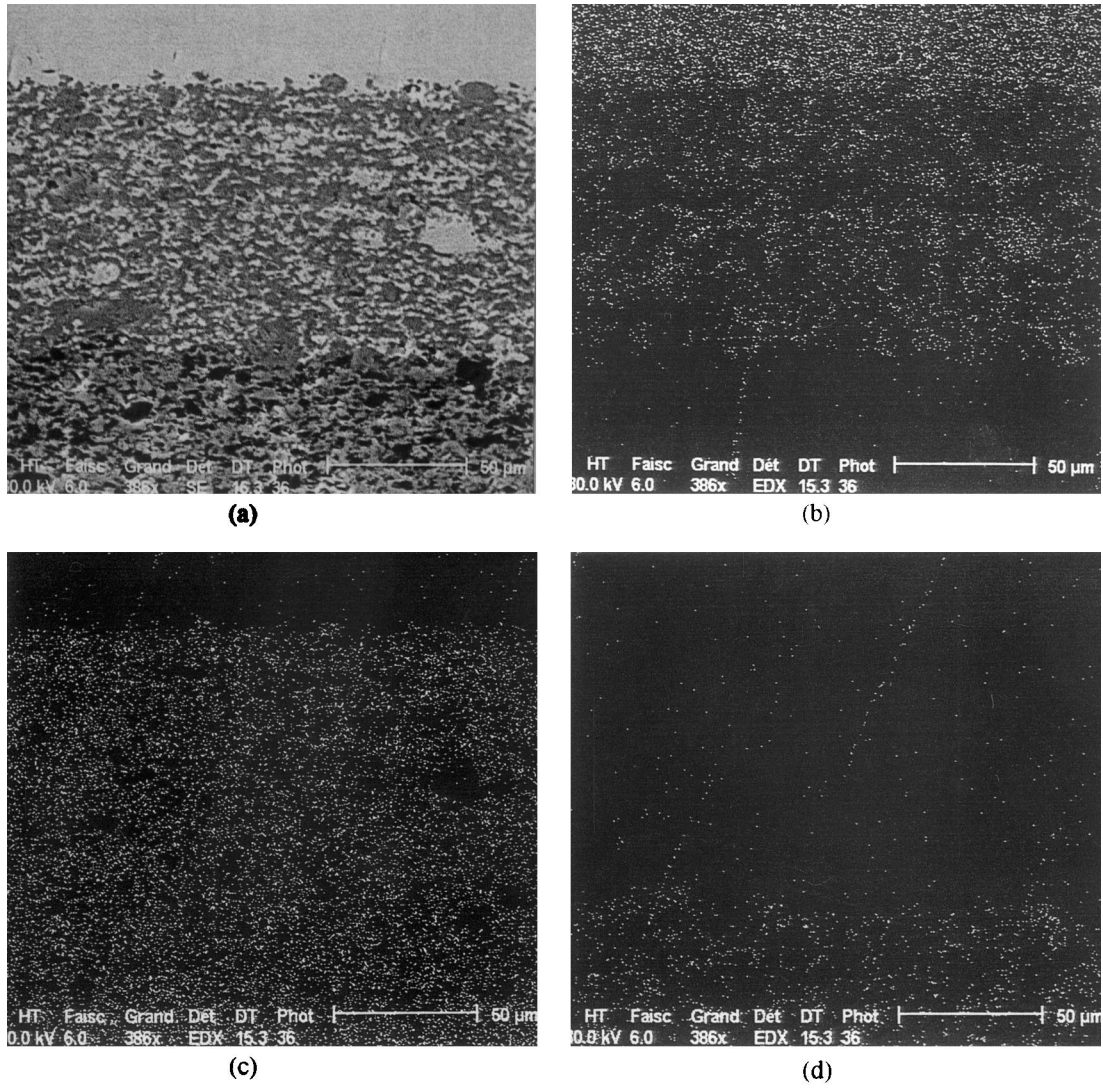


Fig. 6. Microstructure of (a) the steel B/(75%TiN–25%AlN) interface; (b) Fe X-ray map; (c) Ti X-ray map; (d) Al X-ray map.

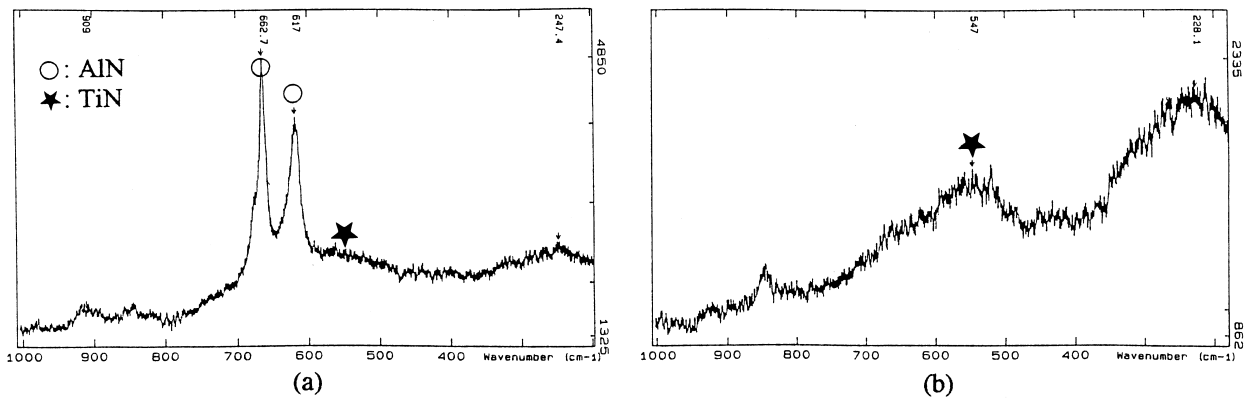
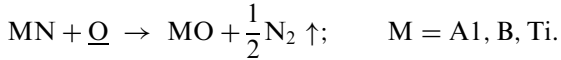


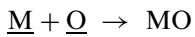
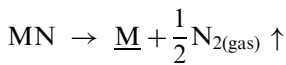
Fig. 7. Raman spectra of (a) 75%TiN–25%AlN substrate and (b) steel B/(75%TiN–25%AlN) interface.

• Direct oxidation of the ceramic by dissolved oxygen according to the following reaction:



Calculation of the Gibbs energy change of these reactions (Table 5) shows that both aluminium and titanium nitrides are unstable against the oxygen dissolved in the steel and, thus, their dissolution is expected. However, dissolution was not observed in TiN even after being in contact with the liquid steel for 1 or 2 h.

• Decomposition of the nitride and oxidation of metallic element¹ according to the following reactions:



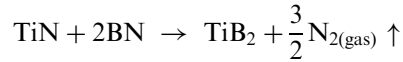
In this case, the calculation of the Gibbs energy change for decomposition of different nitrides shows that in contrast to AlN, the decomposition of TiN is thermodynamically impossible (Table 5). This confirms the corrosion mechanism of AlN and shows that the strong corrosion resistance of TiN is mainly due to its stability under the conditions used in the present work.

4.2. TiN–BN

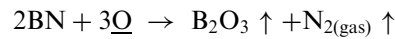
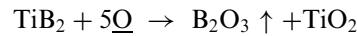
The reaction of TiN with BN explains why the liquid steel spreads on the substrate. The reaction between TiN and BN produces TiB₂ and causes a significant change in the nature of the interface. The presence of TiB₂ and BN in the substrate favours its reaction with

the oxygen dissolved in the liquid steel. The product of the oxidation of TiB are B₂O₃ and TiO₂.^{9,10} As the boron oxide has a high vapour pressure at 1550°C, its spontaneous evaporation allows the development of the oxidation reaction. The corrosion mechanism may be described as below:

• First stage. Reaction between TiN and BN:



• Second stage. Oxidation of BN and TiB₂ by the oxygen dissolved in the steel:



4.3. TiN–AlN

The addition of AlN to TiN modifies the wetting parameters such as contact angle and surface tension. The contact angle increases from 53° for pure TiN to 80° for TiN–50%AlN. The variation of the solid–liquid tension with time for the TiN–AlN substrate indicates a minimum which is characteristic of the occurrence of a chemical reaction at the interface.⁸ SEM and Raman spectroscopy results indicated that corrosion of the TiN–AlN substrate by liquid steel is preceded by preferential attack on AlN grains. This behaviour of the TiN–AlN mixture against the liquid steel may be predicted considering the individual behaviour of TiN and AlN. The corrosion of TiN and AlN may take place through their decomposition. This decomposition is thermodynamically possible in the case of AlN (Table 5),

Table 4
Corroded thickness (in mm) of different ceramic bars in contact with the liquid steel B

	2 h	5 h	10 h	20 h	Observations
AlN pure	0.25	0.8	1.2		Weak attachment
TiN pure	0	0	0	0	Strong attachment, cracking
TiN–10%AlN	0.3	0.4	0.5		Strong attachment, cracking
TiN–25%AlN	0.4	0.55	0.7	2	Strong attachment, cracking
TiN–50%AlN		1.15	1.85	3	Strong attachment, cracking

Table 5
Gibbs energy change of the reactions³

	$\text{MN} + \underline{\text{O}} \rightarrow \text{MO} + \frac{1}{2}\text{N}_2 \uparrow$ ΔG (kJ/mol)		$\text{MN} \rightarrow \underline{\text{M}} + \frac{1}{2}\text{N}_2 \uparrow$ ΔG (kJ/mol)	
Nitrides	1550°C		1570°C	
AlN	–602.13	–601.28	–52.69	–56.15
BN	–401.35	–401.81	35.62	33.19
TiN	–227.14	–225.94	7.28	3.94

but is impossible in the case of TiN. Therefore, in the absence of any reaction between TiN and AlN the corrosion of the TiN–AlN mixture takes place by a preferential attack on AlN grains.

The augmentation of the contact angle by the addition of AlN to TiN seems to contradict the results already reported^{8,11,12} which attribute the chemical interaction in the solid–liquid interface to the variation of the contact angle. According to these results the contact angle between steel and TiN should be higher than that of TiN–AlN due to the lack of any chemical interaction between the liquid steel and TiN and the presence of a chemical interaction in the case of TiN–AlN mixture. This may be explained considering the corrosion mechanism of the TiN–AlN substrate by preferential attack on AlN and its decomposition to aluminium and nitrogen. The aluminium produced is partly oxidised by the oxygen dissolved in the liquid steel giving rise to formation of solid alumina in the steel. The other part of Al is concentrated at the drop surface under the action of convection currents ($\sigma_{AL} < \sigma_{FE}$), and reacts with the residual oxygen of the furnace atmosphere and gives rise to formation of a solid alumina layer on the steel surface which hinders the change of the contact angle.¹ This explains why the contact angle increases by the addition of AlN (Fig. 3). Obviously, the more AlN added to the TiN matrix, the more alumina solid layer is formed at the liquid–vapour interface.

5. Conclusions

The wetting studies on the pure TiN by different steels shows that the contact angle decreases continuously as a function of time without any abrupt change.

The pure TiN indicates a good corrosion resistance against the liquid steels. This behaviour is due to the higher thermodynamic stability of TiN than other nitrides.

The reaction of BN with TiN changes the nature of the initial substrate to TiN–TiB₂–BN that promotes a spontaneous spreading of the liquid steels over the substrate.

The addition of AlN to the TiN matrix decreases the wetting with respect to the pure TiN and pure AlN. However, the contact angle remains less than 90°. The corrosion of the TiN–AlN mixture by the liquid steel takes place by a preferential attack on the AlN grains which are less stable than TiN according to the thermodynamic data.

Acknowledgements

A.A. and S.H.-M. would like to acknowledge Tehran University for financial support.

References

1. Labbe, J. C. and Laïmeche, A., *J. Eur. Ceram. Soc.*, 1996, **16**(8), 893.
2. Amadeh, A., Labbe, J. C., Laïmeche, A. and Quintard, P., *J. Eur. Ceram. Soc.*, 1996, **16**(4), 403.
3. Kubaschewski, O. and Alcock, C. B., *Metallurgical Thermochemistry*, 5th edn. Pergamon Press, 1979.
4. Asano, K., Ishii, A. and Tsutsui, Y., *Taikabutsu Overseas*, 1991, **11**(3), 3.
5. Labbe, J. C., Lachaud-Durand, A., Laïmeche, A., Paulyou, V. and Tétard, D., *High Temp. Chem. Processes*, 1992, **1**, 151.
6. Rhee, S. K., *J. Am. Ceram. Soc.*, 1970, **53**(12), 639.
7. Sangiorgi, R., Muolo, M. L. and Passerone, A., *Mater. Sci. Monogr.*, (*High Tech. Ceram. Pt. A*), 1987, **38A**, 415.
8. Aksay, I. A., Hoge, C. E. and Pask, J. A., *J. Phys. Chem.*, 1974, **78**(12), 1178.
9. Lebugle, A. and Montel, G., *Rev. Int. Htes. Temp. et Réfract.*, 1974, **IV**, 231.
10. Voitovich, R. F. and Pugach, E. A., *Poroshkoyava Metallurgiya*, 1975, **146**(2), 57.
11. Nakae, H., Fujii, H. and Sato, K., *Materials Transactions, JIM*, 1992, **33**(4), 400.
12. Delannay, F., Froyen, L. and Deruyttere, A., *J. Mater. Sci.*, 1987, **22**, 1.